Appl. Phys. A (2015) 119:795–805
DOI 10.1007/s00339-015-9081-8

Applied Physics A
Materials Science & Processing

CrossMark

INVITED PAPER

Neutron activation autoradiography and scanning macro-XRF of Rembrandt van Rijn's *Susanna and the Elders* (Gemäldegalerie Berlin): a comparison of two methods for imaging of historical paintings with elemental contrast

Matthias Alfeld · Claudia Laurenze-Landsberg · Andrea Denker · Koen Janssens · Petria Noble

Received: 13 December 2014 / Accepted: 25 February 2015 / Published online: 14 April 2015
© Springer-Verlag Berlin Heidelberg 2015

Abstract Imaging methods with elemental contrast are of great value for the investigation of historical paintings, as they allow for study of sub-surface layers that provide insight into a painting's creation process. Two of the most important methods are neutron activation autoradiography (NAAR) and scanning macro-XRF (MA-XRF). Given the differences between these methods in the fundamental physical phenomena exploited, a theoretical comparison of their capabilities is difficult and until now a critical comparison of their use on the same painting is missing. In this paper, we present a study of Rembrandt van Rijn's painting *Susanna and the Elders* from the Gemäldegalerie in Berlin employing both techniques. The painting features a considerable number of overpainted features and a wide range of pigments with different elemental tracers, including earth pigments (Mn/Fe), Azurite (Cu), lead white (Pb), vermilion (Hg) and smalt (Co, As). MA-XRF can detect all elements above Si ($Z = 14$), suffers from few spectral overlaps and can be performed in a few tens of hours in situ, i.e. in a museum. NAAR requires the stay of the painting at a research facility for several weeks, and inter-element interferences can be difficult to resolve. Also, only a limited number of elements contribute to the acquired autoradiographs, most notably Mn, Cu, As, Co, Hg and P. However, NAAR provides a higher lateral resolution and is less hindered by absorption in covering layers, which makes it the only method capable of visualizing P in lower paint layers.

M. Alfeld (✉)
Deutsches Elektronen-Synchrotron DESY, Notkestraße 85, 22607 Hamburg, Germany
e-mail: matthias.alfeld@gmx.de

M. Alfeld · K. Janssens
University of Antwerp, Groenenborgerlaan 171, 2020 Antwerp, Belgium

C. Laurenze-Landsberg
Gemäldegalerie Berlin, Stauffenbergstraße 40, 10785 Berlin, Germany

A. Denker
Helmholtz-Zentrum Berlin (formerly Hahn-Meitner-Institute), Hahn-Meitner-Platz 1, 14109 Berlin, Germany

P. Noble
Rijksmuseum, Museumstraat 1, 1070 DN Amsterdam, The Netherlands

1 Introduction

Sub-surface paint layers in historical paintings are of great interest in art-historical studies as they can provide insight into the painting's creation process and the *modus operandi* of the artist. Of special interest are features of a painting's initial or intermediate phases that were subsequently overpainted. As these changes lie below covering paint, completely hidden to visible light, scientific techniques need to be employed for their study.

A standard technique for the investigation of historical paintings is X-ray radiography (XRR). In case of XRR, the intensity of X-rays transmitted through the painting is recorded in a photographic medium or area detector. The radiographs obtained are typically dominated by the heaviest elements present; in case of paintings dating before the twentieth century, this is typically Pb from lead white ($PbCO_3$ and $2PbCO_3{\cdot}Pb(OH)_2$). The study of hidden paint layers containing lighter elements, such as Fe and Mn in earth pigments, is seldom possible. Moreover, since all layers contribute equally to the recorded radiograph, independent of their position in the painting's stratigraphy, it

may contain considerable contributions from the support of the painting.

Images acquired with elemental contrast allow the identification of many pigments and the visualization of additional features. The clear visualization of underlying paint layers is possible, provided pigments of different elemental composition were used in surface and sub-surface layers. The acquisition of such element-specific images of paintings is technically challenging, and for a long time, the only method available for doing so was neutron activation autoradiography (NAAR) [1–7]. Related element-specific methods such as X-ray fluorescence analysis (XRF) and particle-induced X-ray emission (PIXE) have long been used for the analysis of spots and small areas on the surface of paintings [8–12] but did not provide information in the form of large-scale images. Recently, scanning macro-XRF (MA-XRF) was introduced for the acquisition of surface and sub-surface elemental distribution images of large areas (up to several square metres) [13]. The scientific methods available for the study of historical paintings have been subject to two recent review papers. Other methods of depth profiling and sub-surface imaging such as X-ray K-edge imaging and various techniques exploiting IR radiation are reviewed in Ref. [14], while Ref. [15] deals with techniques employing synchrotron radiation.

In NAAR, short-term radioactivity is induced in the painting by means of cold or thermal neutrons emitted by a nuclear research reactor. In selected time windows, the painting is then brought in contact with a photographic medium that is darkened by the emitted β-radiation. By selecting appropriate time windows, autoradiographs dominated by the distribution of different elements are obtained. In the chosen time windows, the intensity of the β-radiation emitted by the radio isotopes of the investigated element is at its maximum relative to that of others, i.e. when radioisotopes with a shorter life time have mostly faded. The appropriate time window for a radioisotope is commonly around its half-life. NAAR allows for the investigation of a broad range of elements present in pigments with the notable exception of Fe (earth pigments) and Pb (lead-based pigments), since no isotopes of these elements are transformed into radioactive equivalents that darken the photographic medium employed. In addition to the detection of the β-radiation by photographic film or image plates, the emitted γ-radiation can be recorded with an energy dispersive detector to clearly identify the isotopes that are darkening the photographic medium. The fact that NAAR requires the transport of the painting to a research reactor and necessitates a stay of a few weeks constitutes a major limitation of the method.

With MA-XRF, the surface of the painting is scanned with a focused or collimated X-ray beam with a diameter of a few hundred micrometres. The X-ray fluorescence radiation emitted from the painting allows for the identification of elements present in surface and, due to the penetrative nature of X-rays, in sub-surface layers as well. XRF is in general suitable for the study of elements heavier than Na ($Z = 11$) in surface layers, but the long air path between painting and detector and the window of the detector limits MA-XRF typically to elements heavier than Si ($Z = 14$), with good results obtained for elements heavier than S ($Z = 16$). The absorption characteristics of covering paint layers determine to what extent elements can be detected in underlying features. In case of thin covering paint layers, elements heavier than Cu ($Z = 29$) can generally be clearly visualized.

The first MA-XRF experiments on paintings exploited the high intensity of synchrotron radiation sources [13, 16, 17], but soon mobile instruments based on X-ray tubes were constructed that achieved comparable results for a broad range of elements [18, 19]. A commercial XRF scanner for the investigation of small areas (5×5 cm^2) was realized several years ago [8], and recently a commercial, mobile instrument for large areas (80×60 cm^2) was developed by Bruker Nano GmbH (Berlin, Germany) [20]. This scanner employs a polycapillary optic to focus the primary beam down to 50 μm, which allows for the acquisition of elemental distribution images with high lateral resolution in the range of the beam size.

XRF is a mature technique for which robust data evaluation procedures have been developed; thus, the overlap of fluorescence lines of different elements can in nearly all cases be resolved.

The mobile instrumentation makes it possible to investigate a painting on the wall of a museum or on an easel in the conservation studio of the museum for easier positioning. Radiation safety is not a significant issue, as the pencil beam used to excite the paint only gives rise to scattered radiation of low intensity. However, care must be taken to avoid direct exposure of humans to the transmitted beam.

XRR, NAAR and MA-XRF are all considered to be non-destructive methods of analysis. In NAAR, only approximately 4 in 10^{12} atoms in the painting become activated and the dose of X-rays absorbed by the painting in XRR and MA-XRF was found to be far below the level to induce any alterations.

NAAR and MA-XRF differ considerably, not only in the fundamental physical phenomena exploited, but also in the way information is recorded. NAAR is a full-field technique that allows investigation of the entire painting simultaneously. MA-XRF, on the other hand, is a scanning technique, and data is acquired in a sequential fashion, pixel by pixel, line by line. With NAAR, the intensity of the emitted β-radiation is "integrated" over a time window

by the photographic medium, while with XRF the photons emitted are detected in an energy dispersive manner and the individual elements that contribute to the XRF spectrum are separated during post-processing. In NAAR, a higher level of darkening of the photographic medium indicates the greater abundance of an element and no spectrometric data are obtained that can be compared to limits of detection calculated for XRF.

In this publication, the greyscale of elemental distribution images acquired by MA-XRF was adjusted to that of XRR and NAAR so that in all images a darker tone indicates a stronger signal.

As a scanning technique, the lateral resolution of MA-XRF is determined by the size of the beam and the step size chosen. As mechanical constraints of a scanning system define a minimum dwell time per pixel, the time available for the experiment does not only affect the contrast obtained, but also affect the lateral resolution. In NAAR, the contrast obtained is dependent on the exposure time of the photographic medium, which cannot be extended indefinitely to minimize overlap with slower decaying isotopes and an overexposure of areas of high concentration. The lateral resolution of NAAR images is dependent on the grain size and thickness of the film employed and the distance between the film and the paint surface, which is influenced by the topography of the painting. Finally, the energy of the emitted β-radiation influences the lateral resolution, as it determines the absorption in the photographic medium.

These fundamental differences between the methods make a theoretical comparison of their capabilities difficult, and a critical comparison of the two methods on the same painting is still missing. Seim et al. have used NAAR and XRF imaging in the investigation of *The Reading Hermit*. The painting is currently attributed to an unknown artist, but the authorship of Rembrandt has been proposed. However, their work focused on the art-historical significance of their findings [21].

In this paper, we compare the results of the two methods—NAAR and MA-XRF—used to investigate Rembrandt van Rijn's *Susanna and the Elders,* signed and dated 1647 (oil on mahogany, 76.6 × 92.8 cm^2, Gemäldegalerie Berlin) as shown in Fig. 1. The painting contains a considerable amount of artist's changes, so-called *pentimenti* (from the Italian verb pentire: "to repent"). Since the first XRR made of this painting in 1931, it is known that an earlier version begun in the second half of the 1630s exists underneath the composition visible today. A drawing made after the earlier version by a pupil of Rembrandt (B. Fabritius (attrb.), c. 1643, Museum of Fine Arts, Budapest) shows features of this earlier version, including the left Elder shown grasping Susanna's breast. The numerous modifications in the composition were described in detail in previous art-historical studies [22–25]. In order to obtain further information about the changes made with pigments other than lead white, the painting was investigated in 1994 with NAAR, which revealed additional hidden details. The painting was chosen for the present comparison of the two techniques, because of its clearly visible *pentimenti*, but also because of its limited dimensions; this allowed the MA-XRF scans to be performed within a single (closed) day at the museum.

2 Experimental

2.1 X-ray radiography (XRR)

The X-ray radiograph of *Susanna and the Elder*s (Fig. 1, right) was made in 2007 by Gerald Schulz, technical photographer at the Gemäldegalerie, with Agfa/GE Strukturix DX4- film, using a Seifert Isovolt X-ray tube operating at 40 kV and 15 mA with an exposure time of 5 min. For this investigation, the painting was brought to the photography department of the museum and removed from public display for one day.

Fig. 1 Rembrandt van Rijn, *Susanna and the Elders*, signed and dated: "Rembrandt.f. 1647", oil on mahogany, 76.6 × 92.8 cm^2 (Gemäldegalerie Berlin, Catalogue Number 828 E), normal light photograph (*left*) and XRR (*right*)

2.2 Neutron activation autoradiography (NAAR)

The NAAR investigations of the painting were carried out in 1994 at the BER II research reactor at the Helmholtz-Zentrum Berlin (formerly the Hahn-Meitner Institute). For activation, the painting was placed on a motorized stage in a dedicated, climate-controlled irradiation room. The neutrons leaving the reactor via a cold neutron guide of 3.5 × 12.5 cm^2 with a flux of 1.1×10^9 cm^{-2} s^{-1} impinged on the surface of the painting in a flat angle (<3) so that a 12.5-cm broad stripe of the painting was irradiated at a time. By moving the painting up and down through the neutron beam, the whole surface of the painting was activated for approximately 3 h. Activation time and exposure times of the photographic medium were based on calculations published elsewhere [7].

After activation, the irradiated painting was brought to a climate-controlled dark room, where the photographic film in close contact with the painting was exposed to the β-radiation emitted from it. The schedule of film exposures, along with the dominant radioisotopes and their respective half-lives, is given in Table 1. The NAAR measurements consisted of five exposures, each composed of six highly sensitive X-ray films (Kodak XAR 5, 35 × 43 cm^2) that required the painting to stay at the nuclear facility for two months. Between the first and second exposure, the elements present in the painting were identified by recording γ-spectra from selected spots of the painting's surface and also the entire painting with a longer acquisition time.

Since in this case, investigation with NAAR was aimed at the acquisition of high contrast images with a precise drawing and enhanced readability and not at the identification of isotopes, it was not attempted to distinguish between ^{56}Mn and the contributions of the two Cu isotopes ^{64}Cu and ^{66}Cu by the use of a thin filter, as described in Ref. [3].

2.3 Scanning macro-XRF (MA-XRF)

For the MA-XRF investigation, after the closing of the museum on Sunday evening, the framed painting was brought to the conservation studio of the museum where it remained until Tuesday morning, when it was taken back to the gallery. Since the picture is on constant public display, investigation of the painting took place in a limited time frame, in this case a total of 38 h. For this reason, the lower left corner of the painting was not scanned. It is important to realize that available time determines the dwell time and therefore the quantity and quality of information.

The macro-XRF scanning of the painting was carried out using an in-house built scanner of the University of Antwerp, shown in Fig. 2. The instrument consists of a 10-W Rh-anode transmission X-ray tube (Moxtek, UT, USA) mounted with four silicon drift (SD) detectors (two Vortex EX-60 and two Vortex EX-90 with an active area of 50 mm^2 each, SII, Northridge, CA, USA) on a motor stage with 60 × 60 cm travel range (Newport Corporation, Irvine, CA, USA). As beam defining optic, a Pb collimator with a diameter of 0.8 mm was used. The detector electronics (DXP-XMAP, XIA LLC, Hayward CA, USA) were set to the relatively short peak shaping time of 0.7 μs in order to reduce the dead time during the acquisition, yielding an energy resolution of 220 eV at the Mn-Kα line (5.9 keV). The primary X-ray beam impinged on the surface at normal incidence, while the fluorescence detectors, positioned at a distance of 2–3 cm, featured detection angles of 45 and 47 degrees.

The characterization of the instrument has been previously described in detail elsewhere [26]. For a broad range of elements [Fe ($Z = 26$) to Mo ($Z = 42$)], a sensitivity of more than 10,000 counts per second and per mass per cent was obtained. As most pigments are present in a painting at a concentration level of several mass per cent, this allows for the acquisition of virtually noise-free elemental distribution images with a dwell time of a fraction of a second.

Three elemental distribution images were acquired with a step size of 1 mm, covering the better part of the painting with the exception of the lower left corner. An additional scan with a vertical step size of 1 mm and a horizontal step

Table 1 Time windows and radioisotopes of strong relative β-activity of the autoradiographs

Autoradiograph	Time after activation	Duration	Strongly β-active radioisotopes	Weakly β-active radioisotopes
01	30 min	2 h	^{56}Mn (2.6 h)	^{64}Cu (12.8 h)
02	6 h 45 min	17 h	^{64}Cu (12.8 h)	^{76}As (26.4 h)
03	1 day 6 h	1 day 18 h	^{76}As (26.4 h)	^{64}Cu (12.8 h)
04	4 days	8 days	^{76}As (26.4 h)	^{32}P (14.3 days), ^{203}Hg (46.6 days), ^{60}Co (5.3 a)
05	12 days	58 days	^{32}P (14.3 days), ^{203}Hg (46.6 days), ^{60}Co (5.3 a)	

Half-life times are in brackets

Fig. 2 MA-XRF scanner during investigation of *Susanna and the Elders* in the conservation studio of the Gemäldegalerie, Berlin

size of 0.6 mm was done to obtain more detailed information about the figure of Susanna and the first Elder.

The elemental distribution images were acquired with tube settings of 45 kV and 0.2 mA, yielding an average count rate of 23,000 counts/s per detector, and dwell times between 0.1 and 0.175 s. For data processing, the spectra acquired by the four detectors were scaled to the same energy and summed. The spectra were processed with the PyMCA software package [27]. Correction of dwell time variations and stitching of the individual scans to one elemental distribution image were done after the acquisition with the *datamuncher* software package [28]. Elements up to Sn ($Z = 50$) were primarily detected by their K-level fluorescence, while heavier elements were detected by their L- and M-level radiation.

2.4 Results and discussion

As can be seen in Fig. 1, XRR already revealed considerable changes to the composition. The adjustments made to the tree in the upper left corner (a in Fig. 1) are obvious: The painting initially featured low buildings and open sky, which was partly obstructed by a shape assumed to be a large tree. The background was later filled in with a massive tower. At a later date, the size of the tree was also reduced. In the radiograph, it is also clear to see that the pose of Susanna has been adjusted as well: her left shoulder was originally higher, and the position of the left hand was also changed more than once (b in Fig. 1). As a result of the changes and superimposed paint layers, her body appears less well defined in the radiograph. The originally outstretched arm of the leftmost Elder, reaching for Susanna's breast, is also discernible as it was executed with lead white.

In the upper part of the painting, some bright spots resulting from filled holes in the panel can be seen that were filled with strongly X-ray-absorbing material. Strongly absorbing paint is also present around c in Fig. 1. The bright feature on the left in the radiograph of the painting (d in Fig. 1) is a wax seal on the back of the painting containing the (red) pigment vermilion (HgS).

The radiograph also indicates modifications to the first Elder's headgear, which was originally higher, as well as extensive changes to Susanna's cloak and sash on top of the stone pedestal in the lower right (e, f in Fig. 1).

In the area of Susanna's cloak (f) and the strongly absorbing paint in the upper right corner (c), Sn was found (see Fig. 5). It can be concluded that these features were painted with the pigment lead tin yellow (Pb_2SnO_4 or $Pb(Sn,Si)O_4$) and were later overpainted.

In Fig. 3, the elemental distribution images of Mn and Cu (obtained by MA-XRF) and the autoradiographs 01 and 02 (obtained by NAAR) are shown. While the first autoradiograph is meant to demonstrate the presence of Mn (in brown earth pigments), the second is expected to be dominated by Cu (see Table 1). However, in this painting, both autoradiographs 01 and 02 appear similar. When the corresponding elemental distribution images of Mn and Cu are compared, it can be concluded that Mn is present at a very low concentration level as compared to Cu, yielding a noisy distribution image. This is confirmed by the XRF sum spectrum, shown in Fig. 3 (bottom left) where the net intensity of Mn is of the order of a factor 50 lower than that of Cu, while the XRF sensitivity of both elements is essentially the same. This explains why autoradiograph 01 is dominated by Cu. The Mn is assumed to be present in brown earth pigments applied as a thin underpainting or painted sketch. Based on the information provided by NAAR and MA-XRF, it is not possible to identify which Cu-containing pigment(s) was used; however, based on previous technical studies of Rembrandt paintings, the blue Cu-containing pigment is assumed to be azurite [29]. In autoradiographs 01 and 02, we see that the Cu pigment(s) were used to paint the foliage in the left part of the painting. It is also assumed to be present in a previous version of the sky. The trees in this area are a combination of the Cu-containing pigment and earth pigments (see Fe distribution in Fig. 5). The Cu-containing pigment(s) were also used for the bodice of the earlier version of the robe of the first Elder, and it is also present in the overpainted vegetation in the upper right (c in Fig. 1). In the Cu elemental distribution image, the first Elder's turban also appears smaller. Behind the back of the Elder in the right

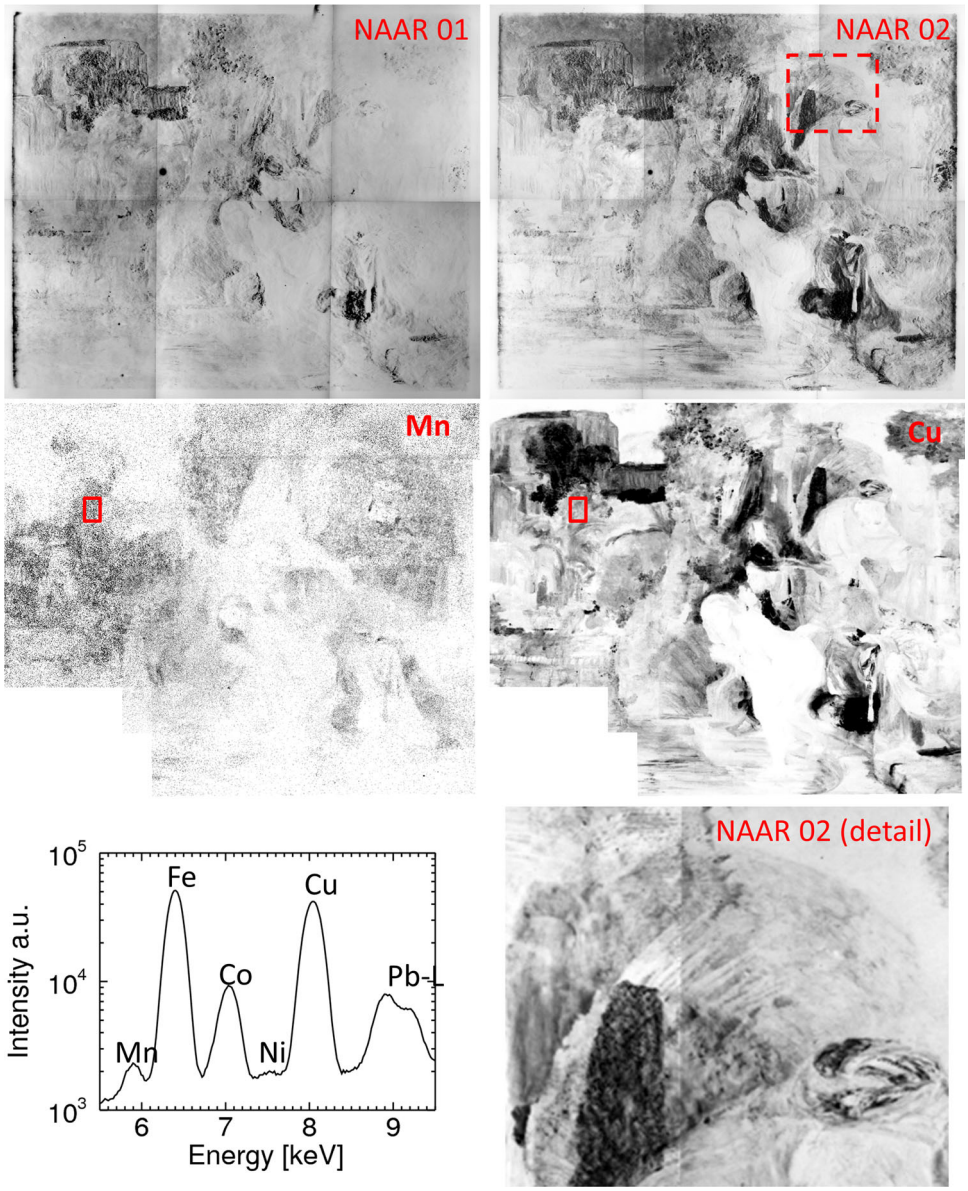

Fig. 3 *Top row* autoradiographs 01 (showing Mn with Cu contributions) and 02 (showing Cu). *Middle row* elemental distribution images of Mn and Cu acquired with MA-XRF. *Bottom row* spectrum showing the sum of all pixels indicated by the *square* in the MA-XRF results (*left*). Rembrandt's scratch marks from the removal of lower paint layers are shown in a detail of autoradiograph 02 (*right*). The location of this detail is indicated by the *dashed square* in the upper right image (*top row*)

background, there was an archway that opened to a view of blue sky. The blue paint was scraped away with a narrow tool, as can be seen in the detail of autoradiograph 02 in Fig. 3 (lower right).

Autoradiograph 03, shown in Fig. 4, shows a decreasing contribution of Cu, whereas the darkening by As has increased. The element As is present in the dark area to the lower right of Susanna's foot, above the cross in the As distribution image in Fig. 4. This is due to Rembrandt's use of smalt, a ground Co-containing K-rich glass, which, depending on the Co ore and manufacturing process, contains notable amounts of other elements, such as As. It is rather striking that Co and As are not correlated in the sky in the upper left corner. This suggests that Rembrandt used two different kinds of smalt for different parts of the paintings. This was already observed in a previous study [30]. Elsewhere in the painting, smalt was not so much used as a blue pigment, but to create a purplish tone of paint in the shadow areas.

The detection of As by MA-XRF in historical paintings is difficult because the K lines of As (As-K_α = 10.53 keV, As-K_β = 11.72 keV) overlap with the L lines of Pb (Pb-L_α = 10.55 keV) and Hg (Hg-L_β = 11.82 keV). If only one of the two elements is present, the intensity of As can still be correctly determined from its overlap free fluorescence line. In spectra with good statistics and with the appropriate detector energy resolution, the contributions of As, Pb and Hg can be correctly separated due to the minor differences in line energy and known line ratios. However, in the experiments described here, each spectrum was

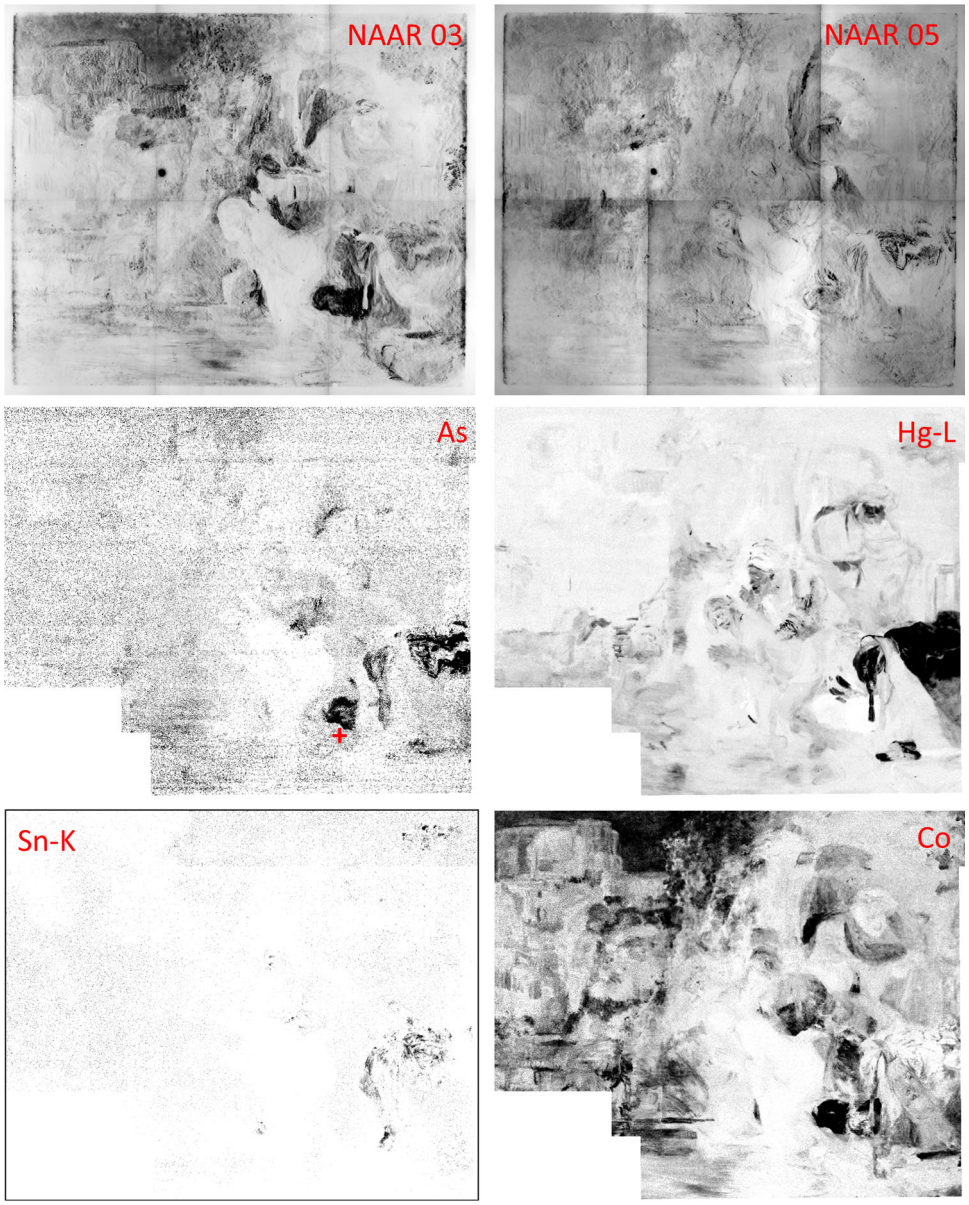

Fig. 4 *Top row* autoradiographs 03 (showing As with Cu contributions) and 05 (showing Co, P and Hg). *Middle row* elemental distribution images of As and Hg acquired by MA-XRF. *Bottom row* elemental distribution images of Sn and Co acquired by MA-XRF. The element P was not detectable by MA-XRF under the chosen experimental conditions

acquired for a fraction of a second so that this is not possible. Due to this overlap, care needs to be taken not to reject all As found in areas with high Pb and Hg abundance, as it is possible that the orange-yellow pigments orpiment (As_2S_3) or realgar (As_4S_4) may have been used to set additional golden accents on the highly decorated earlier version of the first Elder's clothing. To the authors' best knowledge, orpiment has not been identified in Rembrandt paintings and the accents on the Elder's clothes are not apparent in autoradiograph 03, which is sensitive for As. So although the presence of orpiment cannot be excluded based on our investigations, we tend to assume the absence of this pigment in this painting.

The autoradiograph 05 in Fig. 4 is darkened by the isotopes of P, Hg and Co. However, this autoradiograph itself does not provide sufficient information for a clear distinction between these isotopes. To aid interpretation, it is helpful to compare autoradiograph 05 to the elemental distribution images of Hg and Co. This explains many, but not all, features observed. The high intensity of Susanna's cloak, sash and slippers in the Hg elemental image clearly indicates the red used by Rembrandt to paint the final, now visible cloak is the pigment vermilion (HgS); the flesh paints of all the figures also contain a little vermilion, along with details in the left sleeve of the foremost Elder.

Darkening of autoradiograph 05 not caused by Hg and Co can be attributed to P. These considerable contributions are mostly due to the use of bone black, a carbon black-based pigment containing a mixture of $Ca_3(PO_4)_2$, $CaCO_3$ and C, as a remnant of the animal bones burned during its

Fig. 5 Elemental distribution images of Ca, Pb and Fe acquired by MA-XRF

production. For instance, the sketch in bone black for the figure of the second Elder in the background and lines indicating the position of the stairs in the water can be discerned in autoradiograph 05.

In Fig. 5, elemental distribution images of Ca, Pb and Fe are shown. Ca is present in the light-coloured ground of the painting, supposedly in the form of chalk ($CaCO_3$), and is mainly detected in areas with less lead white in the covering layers. Furthermore, it is present in bone black used in dark areas, such as the shadows. Pb is mainly present in lead white and used throughout the painting, mixed with smalt in the sky. Less intense signals were recorded in the areas where lead tin yellow was used. The distribution of lead white in the macro-XRF map is comparable to the radiograph, but shows fewer contributions from the panel support and an inferior lateral resolution. When comparing a radiograph and a macro-XRF distribution image, it is important to remember that dark areas in the latter indicate a high abundance, while the stronger absorption of X-rays results in brighter areas in a radiograph.

Fe is present in yellow and brown earth pigments used to overpaint large sections of the painting. It was also used to model the garden to the left of the figures where it is combined with the Cu pigment in the trees. Contour lines, apparent in autoradiograph 05, are clearly visible suggesting that they were executed with a mixture of pigments, including earth pigments and bone black.

In Fig. 6, visible light photography, XRR, NAAR and MA-XRF results of Susanna and the first Elder are shown. The figure of Susanna in both the Pb-L and Hg-L images and the radiograph clearly reveals the adjustment of her pose, especially of her left hand. The element Ca emits fluorescence radiation of low energy so that its elemental distribution image is in agreement with the visual impression of the final version of the painting. If the Hg distribution is superimposed on the Ca distribution, the repositioning of Susanna's hand is clearly visible. Also the right hand of the first Elder has been modified and was originally either open or positioned slightly higher. Although some contributions of Hg are visible in autoradiograph 05, the above-mentioned modifications are less apparent than in the elemental distribution images acquired by MA-XRF. Both the radiograph and the Pb-L and Cu-K elemental maps reveal a much larger reserve for Susanna's hair, suggesting her hair was initially intended to hang loose.

The repositioning of the Elder's right hand can be discerned in autoradiograph 02, as the reserve left for its initially intended position is discernible.

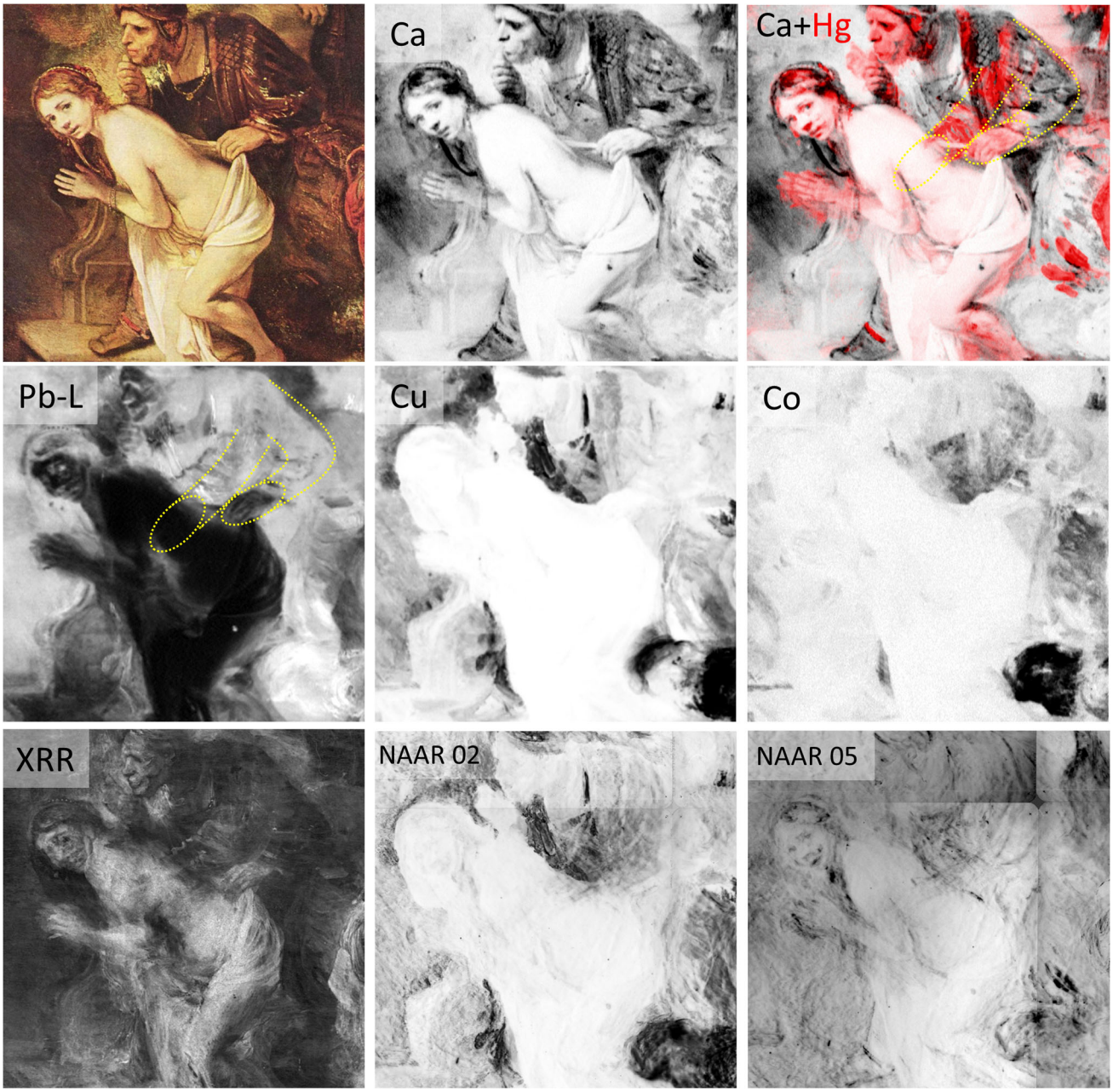

Fig. 6 Details of Susanna and the first Elder: normal light photography (*top left*), XRR (*bottom left*), autoradiographs 02 and 05 and elemental distribution images acquired by MA-XRF. The *dotted yellow lines* in the Hg-L and Pb-L map trace the original and final position of the Elder's arm

The Hg distribution allows us to trace the original position of the first Elder's sleeve, which was painted with red accents. The original and final positions of the arm are indicated by yellow lines. Also in the XRR and Pb-L distribution images, lines indicating the position of the first Elder's arm are discernible. However, if the position of the sleeve in the Hg distribution image is compared to the Pb distribution image, their positions do not agree. It is currently unclear (1) whether the arm was finished in three different positions, (2) whether the line is the remnant of an intermediate sketch or (3) the result of decorations on the clothing of the first Elder. This and other questions still need to be clarified through thorough evaluation of the autoradiographs together with microscopic examination of the painting.

3 Conclusion

Rembrandt van Rijn's *Susanna and the Elders* from the collection of Gemäldegalerie Berlin has been investigated by X-ray radiography (XRR), neutron activation autoradiography (NAAR) and scanning macro-XRF (MA-XRF). The aim of this comparison was to highlight strength and weaknesses of all three methods. All methods were capable of revealing considerable *pentimenti* in the painting.

In the results obtained by XRR, which are dominated by the Pb distribution, many *pentimenti* are visible, but given the complex genesis of the painting, their identification in the radiograph is not straightforward.

Autoradiographs acquired by NAAR provide complimentary information to XRR as they exploit a different contrast mechanism. NAAR is a very suitable tool for the study of pigments such as bone black (P), umber (Mn), copper-based greens and blues (Cu) and vermilion (Hg) due to their susceptibility to activation, but is not capable of visualizing Ca, Fe and Pb. The distribution of an element can be interfered from the autoradiographs, but as all elements contribute simultaneously to the autoradiograph with changing relative intensities, it is feasible that an element present in high abundance dominates one autoradiograph, while other elements of higher relative β-activity but lesser abundance are only weakly discernible, as it is the case for Cu and Mn in Fig. 3. The gamma spectra acquired between the exposures do allow for identification of the elements present, if the areas in question were investigated.

The elemental distribution images acquired by MA-XRF are easier to interpret, mainly because the individual elements are clearly separated, with the exception of As, which is difficult to determine in the presence of Hg and Pb due to spectral overlap. MA-XRF also allows for the study of a broader range of elements as compared to NAAR. However, MA-XRF is not suitable for visualizing the distribution of P (bone black) in sub-surface layers, e.g. sketches. However, P can be detected on the surface of a painting.

Under the chosen experimental conditions, the lateral resolution achieved by XRR and NAAR film was considerably higher than that of MA-XRF. With XRR and NAAR, single brush strokes can be discerned, which can be important for the study of the painting technique employed. However, the lateral resolution achieved in this study by MA-XRF is not a fundamental limitation of the method, but a result of the instrument chosen and the comparably short time period available for investigating the painting. More advanced scanners allow for acquisition of elemental distribution images with a lateral resolution down to 50 μm.

MA-XRF is considerably more surface sensitive than NAAR and XRR. Most signals recorded in the MA-XRF experiments (with the exception of Sn-K) had an energy below 20 keV, and more than 95 % of this radiation would have been absorbed in a 50-μm-thick Pb foil. A Pb foil of this thickness is the equivalent of a 170-μm lead white paint layer, assumed to consist of 80 mass per cent $PbCO_3$ mixed with 20 % of linseed oil ($C_{18}H_{30}O_2$).

NAAR is also affected by absorption in surface layers, but to a considerably lesser degree than MA-XRF. A 50-μm Pb foil would only stop β-radiation with an energy of less than 0.25 MeV so that most elements detected in this work by NAAR would be detected slightly attenuated. Only ^{203}Hg features β-radiation with an energy below this threshold and would thus probably no longer be visible [3]. The reduced effect of absorption in covering layers between NAAR and MA-XRF is especially clear in Fig. 3, where the Cu in the sky, in the upper left corner of the painting, is clearly visible in autoradiograph 02 and only barely visible in the elemental distribution image of Cu acquired by MA-XRF.

Given the relatively short time and less effort required for MA-XRF investigations, this technique is expected to be applied more frequently in the future than NAAR. However, due to the capability of NAAR to visualize the distribution of certain elements through strongly absorbing covering layers, especially P in the case of Rembrandt paintings, both methods ultimately provide complimentary information.

Acknowledgments This research was supported by the Interuniversity Attraction Poles Programme–Belgian Science Policy (IUAP VI/16). The text also presents the results of GOA "XANES meets ELNES" (Research Fund University of Antwerp, Belgium) and from FWO (Brussels, Belgium) Project Nos. G.0704.08 and G.01769.09. M. Alfeld received from 2009 to 2013 a PhD fellowship of the Research Foundation-Flanders (FWO).

References

1. A. Denker, K. Kleinert, C. Laurenze-Landsberg, M. Reimelt, B. Schröder-Smeibidl, Nucl. Instrum. Methods Phys. Res. Sect. A **651**, 273 (2011)
2. C.-O. Fischer, C. Laurenze-Landsberg, C. Schmidt, K. Slusallek, Restauro **105**, 426 (1999)
3. E.V. Sayre, H.N. Lechtman, Stud. Conserv. **13**, 161 (1968)
4. C.-O. Fischer, M. Gallagher, C. Laurenze, C. Schmidt, K. Slusallek, Nucl. Instrum. Methods Phys. Res. Sect. A **424**, 258 (1999)
5. M.W. Ainsworth, J. Brealey, M.J. Cotter, K. Groen, E. Haverkamp-Begemann, P. Meyers, E.V. Sayre, L. van Zelst, *Art and Autoradiography: Insight Into the Genesis of Paintings by Rembrandt, Van Dyck and Vermeer* (Metropolitan Museum of Art, New York, 1982)
6. C.-O. Fischer, J. Kelch, C. Laurenze, W. Leuther, K. Slusallek, Restauro **94**, 259 (1988)
7. C.-O. Fischer, J. Kelch, C. Laurenze, W. Leuther, K. Slusallek, Kerntechnik **51**, 9 (1987)

8. H. Bronk, S. Röhrs, A. Bjeoumikhov, N. Langhoff, J. Schmalz, R. Wedell, H.-E. Gorny, A. Herold, U. Waldschläger, Fresenius J. Anal. Chem. **371**, 307 (2001)
9. A. Denker, J. Opitz-Coutureau, Nucl. Instrum. Methods Phys. Res. Sect. B **213**, 677 (2004)
10. N. Grassi, Nucl. Instrum. Methods Phys. Res. Sect. B **267**, 825 (2009)
11. G. Van der Snickt, K. Janssens, O. Schalm, C. Aibeo, H. Kloust, M. Alfeld, X-Ray Spectrom. **39**, 103 (2010)
12. G. Van der Snickt, C. Miliani, K. Janssens, B.G. Brunetti, A. Romani, F. Rosi, P. Walter, J. Castaing, W. De Nolf, L. Klaassen, I. Labarque, R. Wittermann, J. Anal. At. Spectrom. **26**, 2216 (2011)
13. J. Dik, K. Janssens, G. Van der Snickt, L. van der Loeff, K. Rickers, M. Cotte, Anal. Chem. **80**, 6436 (2008)
14. M. Alfeld, J.A.C. Broekaert, Spectrochim. Acta Part B **88**, 211 (2013)
15. K. Janssens, M. Alfeld, G. Van der Snickt, W. De Nolf, F. Vanmeert, M. Radepont, L. Monico, J. Dik, M. Cotte, G. Falkenberg, C. Miliani, B.G. Brunetti, Annu. Rev. Anal. Chem. **6**, 399 (2013)
16. M. Alfeld, K. Janssens, K. Appel, B. Thijsse, J. Blaas, J. Dik, Z. Kunsttechnol. Konserv. **25**, 157 (2011)
17. D.L. Howard, M.D. de Jonge, D. Lau, D. Hay, M. Varcoe-Cocks, C.G. Ryan, R. Kirkham, G. Moorhead, D. Paterson, D. Thurrowgood, Anal. Chem. **84**, 3278 (2012)
18. M. Alfeld, K. Janssens, J. Dik, W. De Nolf, G. Van der Snickt, J. Anal. At. Spectrom. **26**, 899 (2011)
19. F.P. Hocquet, H.C. del Castillo, A.C. Xicotencatl, C. Bourgeois, C. Oger, A. Marchal, M. Clar, S. Rakkaa, E. Micha, D. Strivay, Anal. Bioanal. Chem. **399**, 3109 (2011)
20. M. Alfeld, J. Vaz Pedroso, M. van Eikema Hommes, G. Van der Snickt, G. Tauber, J. Blaas, M. Haschke, K. Erler, J. Dik, K. Janssens, J. Anal. At. Spectrom. **28**, 760 (2013)
21. C. Seim, C. Laurenze-Landsberg, B. Schröder-Smeibidl, I. Mantouvalou, C. de Boer, B. Kanngießer, J. Anal. At. Spectrom. **29**, 1354 (2014)
22. M. Franken, in *Album Discipulorum*, ed. by J.R.J. van Asperen de Boer (Waanders, Zwolle, 1997), pp. 66–73
23. M. Franken, in *Rembrandt: Quest of a Genius*, ed. by E. van de Wetering (Waanders, Zwolle, 2006), pp. 153–177
24. E.J. Sluijter, *Rembrandt and the Female Nude* (Amsterdam University Press, Amsterdam, 2006)
25. E. van de Wetering, et al, in *A Corpus of Rembrandt Paintings V*, ed. by E. van de Wetering (Dordrecht, Springer, 2011), pp. 325–342
26. M. Alfeld, G. Van der Snickt, F. Vanmeert, K. Janssens, J. Dik, K. Appel, L. van der Loeff, M. Chavannes, T. Meedendorp, E. Hendriks, Appl. Phys. A Mater. Sci. Process. **111**, 165 (2013)
27. V.A. Sole, E. Papillon, M. Cotte, P. Walter, J. Susini, Spectrochim. Acta Part B **62**, 63 (2007)
28. M. Alfeld, K. Janssens, J. Anal. At. Spectrom. **30**, 777 (2015)
29. D. Bomford, J. Kirby, A. Roy, A. Rüger, R. White, *Art in the Making: Rembrandt* (National Gallery Company, London, 2006), pp. 35–47
30. P. Noble, A. van Loon, M. Alfeld, K. Janssens, J. Dik, Technè **35**, 36 (2012)